

Reconstructing Supersymmetric Theories by Coherent LHC / LC Analyses

B. C. ALLANACH¹, G. A. BLAIR^{2,3}, S. KRAML^{4,5}, H.-U. MARTYN⁶,
G. POLESELLO⁷, W. POROD⁸, AND P. M. ZERWAS²

¹ *LAPTH, Annecy-le-Vieux, France.*

² *Deutsches Elektronen-Synchrotron DESY, D-22603 Hamburg, Germany.*

³ *Royal Holloway University of London, Egham, Surrey. TW20 0EX, UK.*

⁴ *Inst. f. Hochenergiephysik, Österr. Akademie d. Wissenschaften, Vienna, Austria.*

⁵ *CERN, Dept. of Physics, TH Division, Geneva, Switzerland.*

⁶ *I. Physik. Institut, RWTH Aachen, D-52074 Aachen, Germany.*

⁷ *INFN, Sezione di Pavia, Via Bassi 6, Pavia 27100, Italy.*

⁸ *Institut für Theoretische Physik, Universität Zürich, Switzerland.*

Abstract

Supersymmetry analyses will potentially be a central area for experiments at the LHC and at a future e^+e^- linear collider. Results from the two facilities will mutually complement and augment each other so that a comprehensive and precise picture of the supersymmetric world can be developed. We will demonstrate in this report how coherent analyses at LHC and LC experiments can be used to explore the breaking mechanism of supersymmetry and to reconstruct the fundamental theory at high energies, in particular at the grand unification scale. This will be exemplified for minimal supergravity in detailed experimental simulations performed for the Snowmass reference point SPS1a.

1 Physics Base

The roots of standard particle physics are expected to go as deep as the Planck length of 10^{-33} cm where gravity is intimately linked to the particle system. A stable bridge between the electroweak energy scale of 100 GeV and the vastly different Planck scale of $\Lambda_{\text{PL}} \sim 10^{19}$ GeV, and the (nearby) grand unification scale $\Lambda_{\text{GUT}} \sim 10^{16}$ GeV, is provided by supersymmetry. If this scenario is realized in nature, experimental methods must be developed to shed light on the physics phenomena near $\Lambda_{\text{GUT}}/\Lambda_{\text{PL}}$. Among other potential tools, the extrapolation of supersymmetry (SUSY) parameters measured at the LHC and an e^+e^- linear collider with high precision, can play a central rôle [1]. A rich ensemble of gauge and Yukawa couplings, and of gaugino/higgsino and scalar particle masses allows the detailed study of the supersymmetry breaking mechanism and the reconstruction of the physics scenario near the GUT/PL scale.

The reconstruction of physical structures at energies more than fourteen orders above the energies available through accelerators is a demanding task. Not only must a comprehensive picture be delineated near the electroweak scale, but the picture must be drawn, moreover, as precisely as possible to keep the errors small enough so that they do not blow up beyond control when the SUSY parameters are extrapolated over many orders of magnitude. The LHC [2] and a future e^+e^- linear collider (LC) [3] are a perfect tandem for solving such a problem: **(i)** While the colored supersymmetric particles, gluinos and squarks, can be generated with large rates for masses up to 2 to 3 TeV at the LHC, the strength of e^+e^- linear colliders is the comprehensive coverage of the non-colored particles, charginos/neutralinos and sleptons. If the extended Higgs spectrum is light, the Higgs particles can be discovered and investigated at both facilities; heavy Higgs bosons can be produced at the LHC in a major part of the parameter space; at an e^+e^- collider, without restriction, for masses up to the beam energy; **(ii)** If the analyses are performed coherently, the accuracies in measurements of cascade decays at LHC and in threshold production as well as decays of supersymmetric particles at LC complement and augment each other *mutually* so that a high-precision picture of the supersymmetric parameters at the electroweak scale can be drawn. Such a comprehensive and precise picture is necessary in order to carry out the evolution of the supersymmetric parameters to high scales, driven by perturbative loop effects that involve the entire supersymmetric particle spectrum.

Minimal supergravity (mSUGRA) provides us with a scenario within which these general ideas can be quantified. The form of this theory has been developed in great detail, creating a platform on which semi-realistic experimental studies can be performed. Supersymmetry is broken in mSUGRA in a hidden sector and the breaking is transmitted to our eigenworld by gravity [4]. This mechanism suggests, yet does not enforce, the universality of the soft SUSY breaking parameters – gaugino and scalar masses, and trilinear couplings – at a scale that is generally identified with the unification scale. The (relatively) small number of parameters renders mSUGRA a well-constrained system that suggests itself in a natural way as a test ground for coherent experimental analyses at LHC and LC. The procedure will be exemplified for a specific set of parameters, defined as SPS1a among the Snowmass reference points [5].

2 Minimal Supergravity: SPS1a

The mSUGRA Snowmass reference point SPS1a is characterised by the following values [5]:

$$\begin{aligned} M_{1/2} &= 250 \text{ GeV} & M_0 &= 100 \text{ GeV} \\ A_0 &= -100 \text{ GeV} & \text{sign}(\mu) &= + \\ \tan \beta &= 10 \end{aligned} \tag{1}$$

for the universal gaugino mass $M_{1/2}$, the scalar mass M_0 , the trilinear coupling A_0 , the sign of the higgsino parameter μ , and $\tan \beta$, the ratio of the vacuum-expectation values of the two Higgs fields. As the modulus of the Higgsino parameter is fixed at the electroweak scale by requiring radiative electroweak symmetry breaking, μ is finally given by:

$$\mu = 357.4 \text{ GeV} \tag{2}$$

This reference point is compatible with the constraints from low-energy precision data, predicting $\text{BR}(b \rightarrow s\gamma) = 2.7 \cdot 10^{-4}$ and $\Delta[g_\mu - 2] = 17 \cdot 10^{-10}$. The amount of cold dark matter is, with $\Omega_\chi h^2 = 0.18$, on the high side but still compatible with recent WMAP data [6] if evaluated on their own without reference to other experimental results; moreover, only a slight shift in M_0 downwards drives the value to the central band of the data while such a shift does not alter any of the conclusions in this report in a significant way.

The form of the supersymmetric mass spectrum of SPS1a is shown in Fig. 1. In this scenario the squarks and gluinos can be studied very well at the LHC while the non-colored gauginos and sleptons can be analyzed partly at LHC and in comprehensive form at an e^+e^- linear collider operating at a total energy below 1 TeV with high integrated luminosity close to 1 ab^{-1} .

The masses can best be obtained at LHC by analyzing edge effects in the cascade decay spectra. The basic starting point is the identification of the a sequence of two-body decays: $\tilde{q}_L \rightarrow \tilde{\chi}_2^0 q \rightarrow \tilde{\ell}_R \ell q \rightarrow \tilde{\chi}_1^0 \ell \ell q$. This is effected through the detection of an edge structure of the invariant mass of opposite-sign same-flavour leptons from the $\tilde{\chi}_2^0$ decay in events with multi-jets and E_T^{miss} . One can then measure the kinematic edges of the invariant mass distributions among the two leptons and the jet resulting from the above chain, and thus an approximately model-independent determination of the masses of the involved sparticles is obtained. This technique was developed in Refs. [7,8] and is worked out in detail for point SPS1a in Ref. [9]. The four sparticle masses (\tilde{q}_L , $\tilde{\chi}_2^0$, $\tilde{\ell}_R$, and $\tilde{\chi}_1^0$) thus measured are used as an input to additional analyses which rely on the knowledge of the masses of the lighter gauginos in order to extract masses from the observed kinematic structures. Examples are the studies of the decay $\tilde{g} \rightarrow \tilde{b}_1 b \rightarrow \tilde{\chi}_2^0 b b$, where the reconstruction of the gluino and sbottom mass peaks relies on an approximate full reconstruction of the $\tilde{\chi}_2^0$, and the shorter decay chains $\tilde{q}_R \rightarrow q \tilde{\chi}_1^0$ and $\tilde{\chi}_4^0 \rightarrow \ell \ell$, which require the knowledge of the sparticle masses downstream of the cascade. For SPS1a the heavy Higgs bosons can also be searched for in the decay chain: $A^0 \rightarrow \tilde{\chi}_2^0 \tilde{\chi}_2^0 \rightarrow \tilde{\chi}_1^0 \tilde{\chi}_1^0 l^+ l^- l^+ l^-$ [10]. The invariant four-lepton mass depends sensitively on m_{A^0} and $m_{\tilde{\chi}_1^0}$. The same holds true for H^0 . Note however that the main source of the neutralino final states are A^0 decays, and that the two Higgs bosons A^0 and H^0 cannot be discriminated in this channel.

The mass measurements obtained at the LHC are thus very correlated among themselves, and this correlation must be taken into account in the fitting procedure. Another

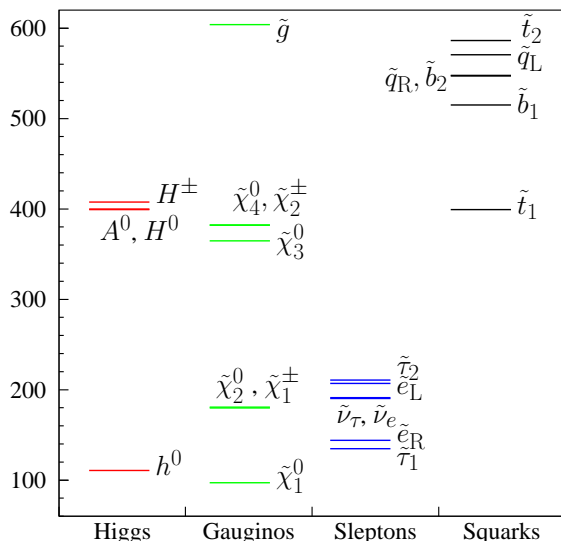


Figure 1: *Spectrum of Higgs, gaugino/higgsino and sparticle masses in the mSUGRA scenario SPS1a; masses in GeV.*

source of correlation comes from the fact that in most cases the uncertainty on the mass measurement is dominated by the systematic uncertainty on the hadronic energy scale of the experiment, which will affect all the measurements involving jets approximately by the same amount and in the same direction.

Two characteristic examples are shown in Fig. 2a: the edge in the di-lepton invariant mass distribution for the decay $\tilde{\chi}_2^0 \rightarrow \tilde{\ell}_R \ell$, and the endpoint of the invariant mass of two leptons plus a jet for the decay $\tilde{q}_L \rightarrow \tilde{\chi}_2^0 q$.

At linear colliders very precise mass values can be extracted from decay spectra and threshold scans [11–13]. The excitation curves for chargino production in S-waves [14] rise steeply with the velocity of the particles near the threshold and thus are very sensitive to their mass values; the same is true for mixed-chiral selectron pairs in $e^+e^- \rightarrow \tilde{e}_R^+ \tilde{e}_L^-$ and for diagonal pairs in $e^-e^- \rightarrow \tilde{e}_R^- \tilde{e}_R^-, \tilde{e}_L^- \tilde{e}_L^-$ collisions [13]. Other scalar sfermions, as well as neutralinos, are produced generally in P-waves, with a somewhat less steep threshold behaviour proportional to the third power of the velocity [13, 15]. Additional information, in particular on the lightest neutralino $\tilde{\chi}_1^0$, can be obtained from decay spectra. Two characteristic examples of a threshold excitation curve and a decay spectrum are depicted in Fig. 2b.

Typical mass parameters and the related measurement errors are presented in Table 1. The column denoted “LHC” collects the errors from the LHC analysis, the column “LC” the errors expected from the LC operating at energies up to 1 TeV with an integrated luminosity of $\sim 1 \text{ ab}^{-1}$. The error estimates are based on detector simulations for the production of the light sleptons, $\tilde{e}_R, \tilde{\mu}_R$ and $\tilde{\tau}_1$, in the continuum. For the light neutralinos and the light chargino threshold scans have been simulated. Details will be given elsewhere; see also Ref. [16]. The expected precision of the other particle masses is taken from Ref. [13], or it is obtained by scaling the LC errors from the previous analysis in Ref. [11], taking into account the fact that the $\tilde{\chi}^0/\tilde{\chi}^\pm$ cascade decays proceed dominantly via τ lep-

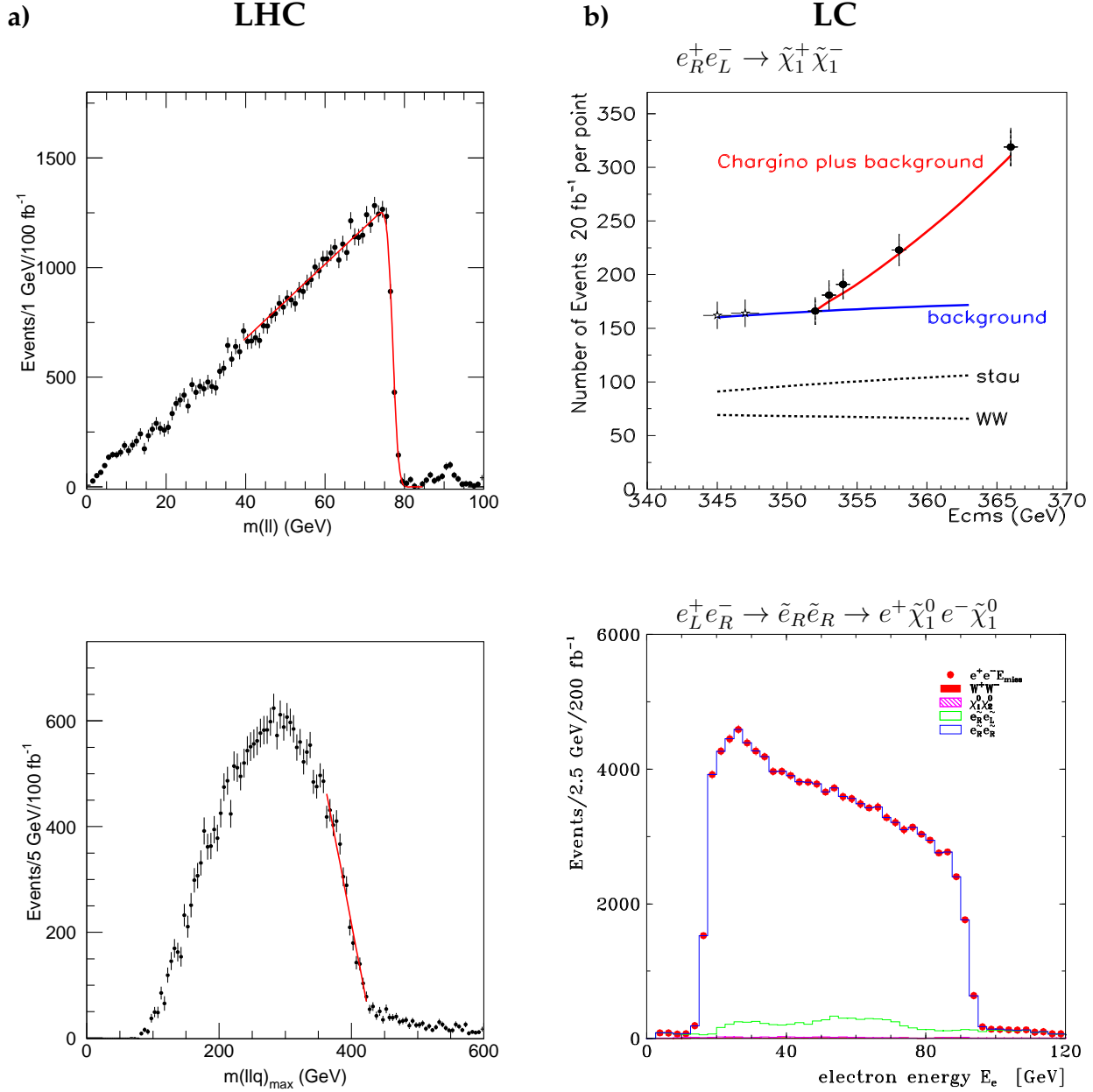


Figure 2: **a) Examples of LHC edge spectra.** *Upper: Two-lepton mass with kinematic edge from the $\tilde{\chi}_2^0$ decay. Lower: Kinematic end-point involving the mass spectrum of two leptons and a jet for \tilde{q}_L decay.* **b) Examples of LC analyses.** *Upper: Threshold scan for chargino production $e_R^+ e_L^- \rightarrow \tilde{\chi}_1^+ \tilde{\chi}_1^-$ including the backgrounds from $W^+ W^-$ and $\tilde{\tau}_1^+ \tilde{\tau}_1^-$; observed event rates correspond to the integrated luminosity $\mathcal{L} = 100 \text{ fb}^{-1}$. Lower: Electron decay spectrum of the continuum reaction $e_L^+ e_R^- \rightarrow \tilde{e}_R^+ \tilde{e}_R^- \rightarrow e^+ \tilde{\chi}_1^0 e^- \tilde{\chi}_1^0$, assuming $\sqrt{s} = 400 \text{ GeV}$ and $\mathcal{L} = 200 \text{ fb}^{-1}$.*

tons in the reference point SPS1a, which is experimentally challenging. The third column of Tab. 1 denoted ‘‘LHC+LC’’ presents the corresponding errors if the experimental analyses are performed coherently, i.e. the light particle spectrum, studied at LC with very high precision, is used as an input set for the LHC analysis.

Mixing parameters must be obtained from measurements of cross sections and polarization asymmetries, in particular from the production of chargino pairs and neutralino pairs [14, 15], both in diagonal or mixed form: $e^+e^- \rightarrow \tilde{\chi}_i^+ \tilde{\chi}_j^-$ [$i, j = 1, 2$] and $\tilde{\chi}_i^0 \tilde{\chi}_j^0$ [$i, j = 1, \dots, A$]. The production cross sections for charginos are binomials of $\cos 2\phi_{L,R}$, the mixing angles rotating current to mass eigenstates. Using polarized electron and positron beams, the cosines can be determined in a model-independent way.

Based on this high-precision information, the fundamental SUSY parameters can be extracted at low energy in analytic form. To lowest order:

$$\begin{aligned}
|\mu| &= M_W [\Sigma + \Delta [\cos 2\phi_R + \cos 2\phi_L]]^{1/2} \\
\text{sign}(\mu) &= [\Delta^2 - (M_2^2 - \mu^2)^2 - 4m_W^2(M_2^2 + \mu^2) \\
&\quad - 4m_W^4 \cos^2 2\beta] / 8m_W^2 M_2 |\mu| \sin 2\beta \\
M_2 &= M_W [\Sigma - \Delta (\cos 2\phi_R + \cos 2\phi_L)]^{1/2} \\
|M_1| &= \left[\sum_i m_{\tilde{\chi}_i^0}^2 - M_2^2 - \mu^2 - 2M_Z^2 \right]^{1/2} \\
|M_3| &= m_{\tilde{g}} \\
\tan \beta &= \left[\frac{1 + \Delta (\cos 2\phi_R - \cos 2\phi_L)}{1 - \Delta (\cos 2\phi_R - \cos 2\phi_L)} \right]^{1/2}
\end{aligned} \tag{3}$$

where $\Delta = (m_{\tilde{\chi}_2^\pm}^2 - m_{\tilde{\chi}_1^\pm}^2) / (4M_W^2)$ and $\Sigma = (m_{\tilde{\chi}_2^\pm}^2 + m_{\tilde{\chi}_1^\pm}^2) / (2M_W^2) - 1$. The signs of $M_{1,3}$ with respect to M_2 follow from measurements of the cross sections for $\tilde{\chi}\tilde{\chi}$ production and gluino processes. In practice one-loop corrections to the mass relations have been used to improve on the accuracy.

The mass parameters of the sfermions are directly related to the physical masses if mixing effects are negligible:

$$m_{\tilde{f}_{L,R}}^2 = M_{L,R}^2 + m_f^2 + D_{L,R} \tag{4}$$

with $D_L = (T_3 - e_f \sin^2 \theta_W) \cos 2\beta m_Z^2$ and $D_R = e_f \sin^2 \theta_W \cos 2\beta m_Z^2$ denoting the D-terms. The non-trivial mixing angles in the sfermion sector of the third generation can be measured in a way similar to the charginos and neutralinos. The sfermion production cross sections for longitudinally polarized e^+ / e^- beams are bilinear in $\cos / \sin 2\theta_{\tilde{f}}$. The mixing angles and the two physical sfermion masses are related to the tri-linear couplings A_f , the higgsino mass parameter μ and $\tan \beta (\cot \beta)$ for down(up) type sfermions by:

$$A_f - \mu \tan \beta (\cot \beta) = \frac{m_{\tilde{f}_1}^2 - m_{\tilde{f}_2}^2}{2m_f} \sin 2\theta_{\tilde{f}} \quad [f : \text{down(up) type}] \tag{5}$$

This relation gives us the opportunity to measure A_f if μ has been determined in the chargino sector.

Accuracies expected for the SUSY Lagrange parameters at the electroweak scale for the reference point SPS1a are shown in Table 2. The errors are presented for the coherent ‘‘LHC+LC’’ analysis. They have been obtained by fitting the LHC observables and

	Mass, ideal	"LHC"	"LC"	"LHC+LC"
$\tilde{\chi}_1^\pm$	179.7		0.55	0.55
$\tilde{\chi}_2^\pm$	382.3	–	3.0	3.0
$\tilde{\chi}_1^0$	97.2	4.8	0.05	0.05
$\tilde{\chi}_2^0$	180.7	4.7	1.2	0.08
$\tilde{\chi}_3^0$	364.7		3-5	3-5
$\tilde{\chi}_4^0$	381.9	5.1	3-5	2.23
\tilde{e}_R	143.9	4.8	0.05	0.05
\tilde{e}_L	207.1	5.0	0.2	0.2
$\tilde{\nu}_e$	191.3	–	1.2	1.2
$\tilde{\mu}_R$	143.9	4.8	0.2	0.2
$\tilde{\mu}_L$	207.1	5.0	0.5	0.5
$\tilde{\nu}_\mu$	191.3	–		
$\tilde{\tau}_1$	134.8	5-8	0.3	0.3
$\tilde{\tau}_2$	210.7	–	1.1	1.1
$\tilde{\nu}_\tau$	190.4	–	–	–
\tilde{q}_R	547.6	7-12	–	5-11
\tilde{q}_L	570.6	8.7	–	4.9
\tilde{t}_1	399.5		2.0	2.0
\tilde{t}_2	586.3		–	
\tilde{b}_1	515.1	7.5	–	5.7
\tilde{b}_2	547.1	7.9	–	6.2
\tilde{g}	604.0	8.0	–	6.5
h^0	110.8	0.25	0.05	0.05
H^0	399.8		1.5	1.5
A^0	399.4		1.5	1.5
H^\pm	407.7	–	1.5	1.5

Table 1: *Accuracies for representative mass measurements at "LHC" and "LC", and in coherent "LHC+LC" analyses for the reference point SPS1a [masses in GeV]. \tilde{q}_L and \tilde{q}_R represent the flavours $q = u, d, c, s$ which cannot be distinguished at LHC. Positions marked by bars cannot be filled either due to kinematical restrictions or due to small signal rates; blank positions could eventually be filled after significantly more investments in experimental simulation efforts than performed until now. The "LHC" and "LC" errors have been derived in Ref. [9] and Ref. [17], respectively, in this document.*

	Parameter, ideal	“LHC+LC” errors
M_1	101.66	0.08
M_2	191.76	0.25
M_3	584.9	3.9
μ	357.4	1.3
$M_{L_1}^2$	$3.8191 \cdot 10^4$	82.
$M_{E_1}^2$	$1.8441 \cdot 10^4$	15.
$M_{Q_1}^2$	$29.67 \cdot 10^4$	$0.32 \cdot 10^4$
$M_{U_1}^2$	$27.67 \cdot 10^4$	$0.86 \cdot 10^4$
$M_{D_1}^2$	$27.45 \cdot 10^4$	$0.80 \cdot 10^4$
$M_{L_3}^2$	$3.7870 \cdot 10^4$	360.
$M_{E_3}^2$	$1.7788 \cdot 10^4$	95.
$M_{Q_3}^2$	$24.60 \cdot 10^4$	$0.16 \cdot 10^4$
$M_{U_3}^2$	$17.61 \cdot 10^4$	$0.12 \cdot 10^4$
$M_{D_3}^2$	$27.11 \cdot 10^4$	$0.66 \cdot 10^4$
$M_{H_1}^2$	$3.25 \cdot 10^4$	$0.12 \cdot 10^4$
$M_{H_2}^2$	$-12.78 \cdot 10^4$	$0.11 \cdot 10^4$
A_t	-497.	9.
$\tan \beta$	10.0	0.4

Table 2: *The extracted SUSY Lagrange mass and Higgs parameters at the electroweak scale in the reference point SPS1a [mass units in GeV].*

the masses of SUSY particles and Higgs bosons accessible at a 1 TeV Linear Collider. For the fit the programs SPheno2.2.0 [18] and MINUIT96.03 [19] have been used. The electroweak gaugino and higgs/higgsino parameters cannot be determined individually through mass measurements at the LHC as the limited number of observable masses leaves this sector in the SPS1a system under-constrained. Moreover, the Lagrange mass parameters in the squark sector can be determined from the physical squark masses with sufficient accuracy only after the LHC mass measurements are complemented by LC measurements in the chargino/neutralino sector; this information is necessary as the relation between the mass parameters is affected by large loop corrections.

3 Reconstruction of the Fundamental SUSY Theory

As summarized in the previous section, the minimal supergravity scenario mSUGRA is characterized by the universal gaugino parameter $M_{1/2}$, the scalar mass parameter M_0 and the trilinear coupling A_0 , all defined at the grand unification scale. These parameters are complemented by the sign of the higgs/higgsino mixing parameter μ , with the modulus determined by radiative symmetry breaking, and the mixing angle, $\tan \beta$, in the Higgs sector.

The fundamental mSUGRA parameters at the GUT scale are related to the low-energy parameters at the electroweak scale by supersymmetric renormalization group transfor-

mations (RG) [20,21] which to leading order generate the evolution for

$$\text{gauge couplings} \quad : \quad \alpha_i = Z_i \alpha_U \quad (5)$$

$$\text{gaugino mass parameters} \quad : \quad M_i = Z_i M_{1/2} \quad (6)$$

$$\text{scalar mass parameters} \quad : \quad M_j^2 = M_0^2 + c_j M_{1/2}^2 + \sum_{\beta=1}^2 c'_{j\beta} \Delta M_\beta^2 \quad (7)$$

$$\text{trilinear couplings} \quad : \quad A_k = d_k A_0 + d'_k M_{1/2} \quad (8)$$

The index i runs over the gauge groups $i = SU(3), SU(2), U(1)$. To leading order, the gauge couplings, and the gaugino and scalar mass parameters of soft-supersymmetry breaking depend on the Z transporters with

$$Z_i^{-1} = 1 + b_i \frac{\alpha_U}{4\pi} \log \left(\frac{M_U}{M_Z} \right)^2 \quad (10)$$

and $b[SU_3, SU_2, U_1] = -3, 1, 33/5$; the scalar mass parameters depend also on the Yukawa couplings h_t, h_b, h_τ of the top quark, bottom quark and τ lepton. The coefficients c_j [$j = L_l, E_l, Q_l, U_l, D_l, H_{1,2}; l = 1, 2, 3$] for the slepton and squark doublets/singlets of generation l , and for the two Higgs doublets are linear combinations of the evolution coefficients Z ; the coefficients $c'_{j\beta}$ are of order unity. The shifts ΔM_β^2 are nearly zero for the first two families of sfermions but they can be rather large for the third family and for the Higgs mass parameters, depending on the coefficients Z , the universal parameters $M_0^2, M_{1/2}$ and A_0 , and on the Yukawa couplings h_t, h_b, h_τ . The coefficients d_k of the trilinear couplings A_k [$k = t, b, \tau$] depend on the corresponding Yukawa couplings and they are approximately unity for the first two generations while being $O(10^{-1})$ and smaller if the Yukawa couplings are large; the coefficients d'_k , depending on gauge and Yukawa couplings, are of order unity. Beyond the approximate solutions shown explicitly, the evolution equations have been solved numerically in the present analysis to two-loop order [21] and threshold effects have been incorporated at the low scale [22]. The 2-loop effects as given in Ref. [23] have been included for the neutral Higgs bosons and the μ parameter.

3.1 Gauge Coupling Unification

Measurements of the gauge couplings at the electroweak scale support very strongly the unification of the couplings at a scale $M_U \simeq 2 \times 10^{16}$ GeV [24]. The precision, being at the per-cent level, is surprisingly high after extrapolations over fourteen orders of magnitude in the energy from the electroweak scale to the grand unification scale M_U . Conversely, the electroweak mixing angle has been predicted in this approach at the per-mille level. The evolution of the gauge couplings from low energy to the GUT scale M_U is carried out at two-loop accuracy. The gauge couplings g_1, g_2, g_3 and the Yukawa couplings are calculated in the \overline{DR} scheme by adopting the shifts given in Ref. [22]. These parameters are evolved to M_U using 2-loop RGEs [21]. At 2-loop order the gauge couplings do not meet exactly [25], the differences attributed to threshold effects at the unification scale M_U which leave us with an ambiguity in the definition of M_U . In this report we define M_U as the scale, *ad libitum*, where $\alpha_1 = \alpha_2$, denoted α_U , in the RG evolution. The non-zero difference $\alpha_3 - \alpha_U$ at this scale is then accounted for by threshold effects of particles with masses of order M_U . The quantitative evolution implies important constraints on the particle content at M_U [26].

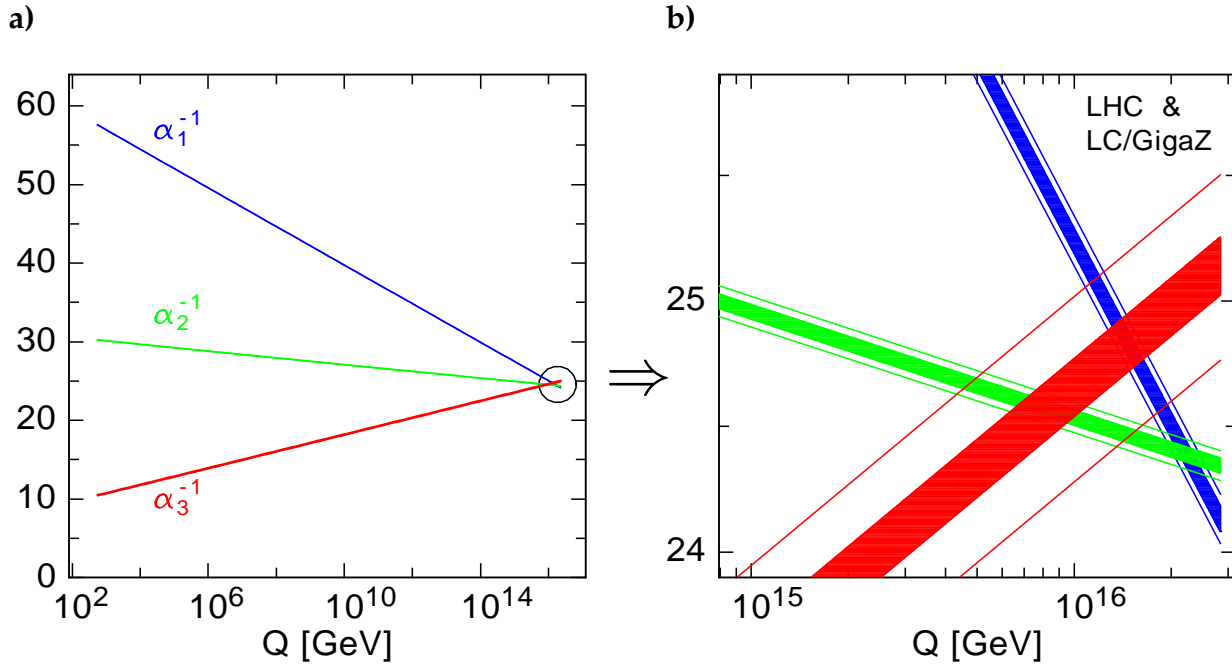


Figure 3: (a) Running of the inverse gauge couplings from low to high energies. (b) Expansion of the area around the unification point M_U defined by the meeting point of α_1 with α_2 . The wide error bands are based on present data, and the spectrum of supersymmetric particles from LHC measurements within mSUGRA. The narrow bands demonstrate the improvement expected by future GigaZ analyses and the measurement of the complete spectrum at “LHC+LC”.

	Present/“LHC”	GigaZ/“LHC+LC”
M_U	$(2.36 \pm 0.06) \cdot 10^{16}$ GeV	$(2.360 \pm 0.016) \cdot 10^{16}$ GeV
α_U^{-1}	24.19 ± 0.10	24.19 ± 0.05
$\alpha_3^{-1} - \alpha_U^{-1}$	0.97 ± 0.45	0.95 ± 0.12

Table 3: Expected errors on M_U and α_U for the mSUGRA reference point, derived for the present level of accuracy and compared with expectations from GigaZ [supersymmetric spectrum as discussed in the text]. Also shown is the difference between α_3^{-1} and α_U^{-1} at the unification point M_U .

Based on the set of low-energy gauge and Yukawa parameters $\{\alpha(m_Z), \sin^2 \theta_W, \alpha_s(m_Z), Y_t(m_Z), Y_b(m_Z), Y_\tau(m_Z)\}$ the evolution of the inverse couplings α_i^{-1} [$i = U(1), SU(2), SU(3)$] is depicted in Fig 3. The evolution is performed for the mSUGRA reference point defined above. Unlike earlier analyses, the low-energy thresholds of supersymmetric particles can be calculated in this framework exactly without reference to effective SUSY scales. The outer lines in Fig. 3b correspond to the present experimental accuracy of the gauge couplings [27]: $\Delta\{\alpha^{-1}(m_Z), \sin^2 \theta_W, \alpha_s(m_Z)\} = \{0.03, 1.7 \cdot 10^{-4}, 3 \cdot 10^{-3}\}$, and the spectrum of supersymmetric particles from LHC measurements complemented in the top-down approach for mSUGRA. The full bands demonstrate the improvement for the absolute errors $\{8 \cdot 10^{-3}, 10^{-5}, 10^{-3}\}$ after operating GigaZ [28,29] and inserting the complete spectrum from “LHC+LC” measurements. The expected accuracies in M_U and α_U are summarized in the values given in Tab. 3. The gap between α_U and α_3 is bridged by contributions from high scale physics. Thus, for a typical set of SUSY parameters, the evolution of the gauge couplings from low to high scales leads to a precision of 1.5 per-cent for the Grand Unification picture.

3.2 Gaugino and Scalar Mass Parameters: Top-down Approach

The structure of the fundamental supersymmetric theory is assumed, in the top-down approach, to be defined uniquely at a high scale. In mSUGRA the set of parameters characterizing the specific form of the theory includes, among others, the scalar masses M_0 and the gaugino masses $M_{1/2}$. These universal parameters are realized at the grand unification point M_U . Evolving the parameters from the high scale down to the electroweak scale leads to a comprehensive set of predictions for the masses, mixings and couplings of the physical particles. Precision measurements of these observables can be exploited to determine the high-scale parameters $M_0, M_{1/2}$, etc., and to perform consistency tests of the underlying form of the theory. The small number of fundamental parameters, altogether five in mSUGRA, gives rise to many correlations between a large number of experimental observables. They define a set of *necessary consistency conditions* for the realization of the specific fundamental theory in nature.

Interludium: In addition to the experimental errors, theoretical uncertainties must be taken into account. They are generated by truncating the perturbation series for the evolution of the fundamental parameters in the \overline{DR} scheme from the GUT scale to a low SUSY scale \tilde{M} near the electroweak scale, and for the relation between the parameters at this point to the on-shell physical mass parameters, for instance. Truncating these series in one- to two-loop approximations leads to a residual \tilde{M} dependence that would be absent from the exact solutions and may therefore be interpreted as an estimate of the neglected higher-order effects.

We estimate these effects by varying \tilde{M} between the electroweak scale and 1 TeV. The theoretical uncertainties of the physical masses and LHC observables derived in this way are listed in Tables 4 and 5, respectively. They are of similar size as the differences found by comparing the observables with different state-of-the-art codes for the spectra [30]. The comparison of the present theoretical uncertainties with the experimental errors at LHC demonstrates that the two quantities do match *cum grano salis* at the same size. Since LC experiments will reduce the experimental errors roughly by an order of magnitude, considerable theoretical efforts are needed in the future to reduce Δ_{th} to a level

Particle	Δ_{th} [GeV]	Particle	Δ_{th} [GeV]
$\tilde{\chi}_1^+$	1.2	\tilde{q}_R	8.4
$\tilde{\chi}_2^+$	2.8	\tilde{q}_L	9.1
$\tilde{\chi}_1^0$	0.34	\tilde{t}_1	4.4
$\tilde{\chi}_2^0$	1.1	\tilde{t}_2	8.3
$\tilde{\chi}_3^0$	0.6	\tilde{b}_1	7.4
$\tilde{\chi}_4^0$	0.3	\tilde{b}_2	8.2
\tilde{e}_R	0.82	\tilde{g}	1.2
\tilde{e}_L	0.31	h^0	1.2
$\tilde{\nu}_e$	0.24	H^0	0.7
$\tilde{\tau}_1$	0.59	A^0	0.7
$\tilde{\tau}_2$	0.30	H^+	1.0
$\tilde{\nu}_\tau$	0.25		

Table 4: Theoretical errors of the SPS1a mass spectrum, calculated as difference between the minimal and the maximal value of the masses if the scale \tilde{M} is varied between 100 GeV and 1 TeV.

	m_{ll}^{max}	m_{llq}^{max}	m_{llq}^{min}	m_{lq}^{high}	m_{lq}^{low}	$m_{\tau\tau}^{max}$	$m_{ll}^{max}(\tilde{\chi}_4^0)$	m_{llb}^{min}
SPheno 2.2.0	80.64	454.0	216.8	397.2	325.6	83.4	283.4	195.9
Δ_{exp}	0.08	4.5	2.6	3.9	3.1	5.1	2.3	4.1
Δ_{th}	0.72	8.1	3.6	7.7	5.5	0.8	0.7	2.9

	$m_{\tilde{q}_R} - m_{\tilde{\chi}_1^0}$	$m_{\tilde{l}_L} - m_{\tilde{\chi}_1^0}$	$m_{\tilde{g}} - m_{\tilde{b}_1}$	$m_{\tilde{g}} - m_{\tilde{b}_2}$	$m_{\tilde{g}} - 0.99 m_{\tilde{\chi}_1^0}$	m_{h^0}
SPheno 2.2.0	450.3	110.0	88.9	56.9	507.8	110.8
Δ_{exp}	10.9	1.6	1.8	2.6	6.4	0.25
Δ_{th}	8.1	0.23	6.8	7.6	1.3	1.2

Table 5: LHC observables assumed for SPS1a and their experimental (Δ_{exp}) and present theoretical (Δ_{th}) uncertainties. [All quantities in GeV].

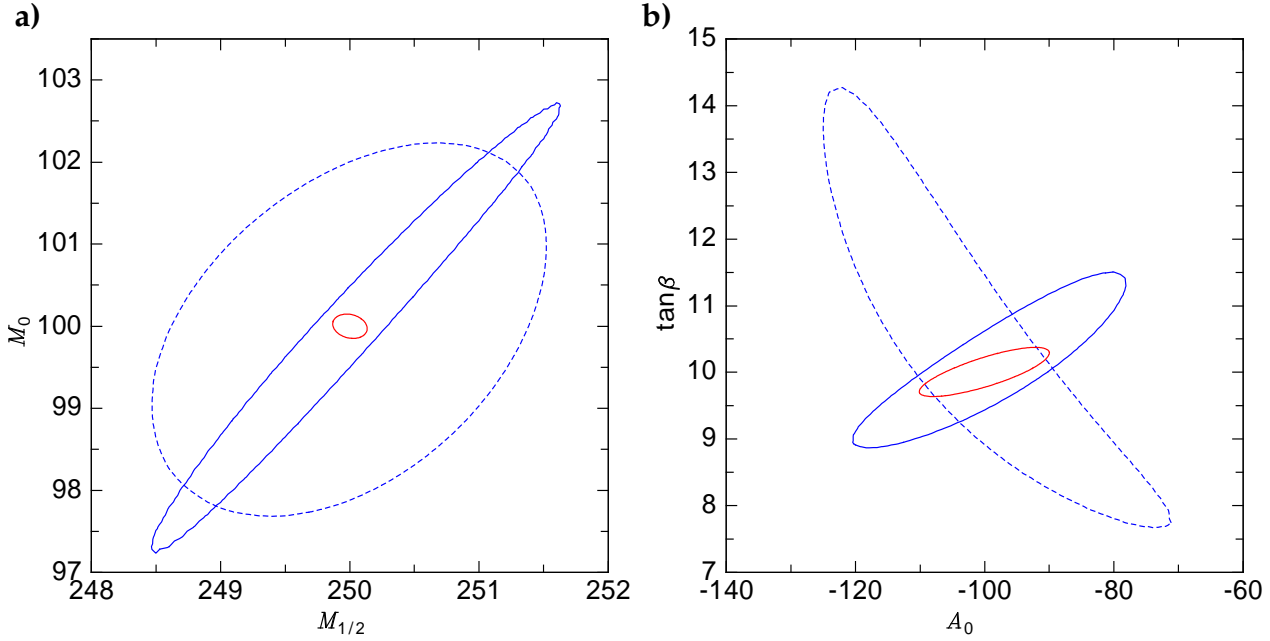


Figure 4: $1\text{-}\sigma$ error ellipses for the mSUGRA parameters in the top-down approach [i.e. the contours of $\Delta\chi^2 = 4.7$ in the $M_0 - M_{1/2}$ and $\tan\beta - A_0$ planes with the respective other parameters fixed to their best fit values, c.f. Table 6]. The full blue ellipses are the results obtained from LHC measurements alone while the red ones are for the combined “LHC+LC” analyses. The dashed blue lines show the results for the “LHC” case including today’s theoretical uncertainties.

that matches the expected experimental precision at LC. Only then we can deepen our understanding of the underlying supersymmetric theory by tapping the full experimental potential of “LC” and of the combined “LHC+LC” analyses.

In the top-down approach, models of SUSY-breaking are tested by fitting their high-scale parameters to experimental data. The minimum χ^2 of the fit gives a measure of the probability that the model is wrong. The results of such a fit of mSUGRA to anticipated “LHC”, “LC”, and “LHC+LC” measurements are shown in Table 6 and Fig. 4. For the “LHC” case the observables in Table 5 have been used, for the LC the masses in Table 1 and for “LHC+LC” the complete information have been used. If mSUGRA is assumed to be the underlying supersymmetric theory, the universal parameters $M_{1/2}$ and M_0 can be determined at the LHC at the per-cent level. LC experiments and coherent “LHC+LC” analyzes improve the accuracy by an order of magnitude, thus allowing for much more powerful tests of the underlying supersymmetric theory. Table 6 takes only experimental errors into account. The accuracy of the present theoretical calculations matches the errors of the “LHC” analysis and can thus be included in a meaningful way in a combined experimental plus theoretical error analysis. Adding Δ_{th} and Δ_{exp} quadratically the errors of the “LHC” analysis increases to: $\Delta M_{1/2} = 2.7$ GeV, $\Delta M_0 = 2.9$ GeV, $\Delta A_0 = 51$ GeV, and $\Delta \tan\beta = 5$. As argued above, significant theoretical improvements by an order of magnitude, i.e. “the next loop”, are necessary to exploit fully the “LC” and “LHC+LC” potential.

The minimum χ^2 of the fit to mSUGRA as in Table 6 is indeed small, $\chi^2_{min}/n.d.o.f. \leq 0.34$ for “LHC”, “LC”, as well as “LHC+LC”. When fitting instead mGMSB model param-

	“LHC”	“LC”	“LHC+LC”
$M_{1/2}$	250.0 ± 2.1	250.0 ± 0.4	250.0 ± 0.2
M_0	100.0 ± 2.8	100.0 ± 0.2	100.0 ± 0.2
A_0	-100.0 ± 34	-100.0 ± 27	-100.0 ± 14
$\tan \beta$	10.0 ± 1.8	10.0 ± 0.6	10.0 ± 0.4

Table 6: Results for the high scale parameters in the top-down approach including the experimental errors.

eters as an alternative to the same data, we would obtain $\chi^2_{min}/14 d.o.f. = 68$ from LHC data alone. Such a result would clearly disfavour this model.

3.3 Gaugino and Scalar Mass Parameters: Bottom-up Approach

In the bottom-up approach the fundamental supersymmetric theory is reconstructed at the high scale from the available *corpus* of experimental data without any theoretical prejudice. This approach exploits the experimental information to the maximum extent possible and reflects an undistorted picture of our understanding of the basic theory.

At the present level of preparation in the “LHC” and “LC” sectors, such a program can only be carried out in coherent “LHC+LC” analyses while the separate information from either machine proves insufficient. The results for the evolution of the mass parameters from the electroweak scale to the GUT scale M_U are shown in Fig. 5.

On the left of Fig. 5a the evolution is presented for the gaugino parameters M_i^{-1} , which clearly is under excellent control for the coherent “LHC+LC” analyses, while “LHC” [and “LC”] measurements alone are insufficient for the model-independent reconstruction of the parameters and the test of universality in the $SU(3) \times SU(2) \times U(1)$ group space. The error ellipse for the unification of the gaugino masses in the final analysis is depicted on the right of Fig. 5a. Technical details of the “LHC+LC” analysis can be found in Ref. [1].

In the same way the evolution of the scalar mass parameters can be studied, presented in Figs. 5b separately for the first/second and the third generation in “LHC+LC” analyses. Compared with the slepton parameters, the accuracy deteriorates for the squark parameters, and for the Higgs mass parameter $M_{H_2}^2$. The origin of the differences between the errors for slepton and squark/Higgs mass parameters can be traced back to the numerical size of the coefficients in Eqs. (8). Typical examples, evaluated at $Q = 500$ GeV, read as follows [1]:

$$M_{\tilde{L}_1}^2 \simeq M_0^2 + 0.47M_{1/2}^2 \quad (11)$$

$$M_{\tilde{Q}_1}^2 \simeq M_0^2 + 5.0M_{1/2}^2 \quad (12)$$

$$M_{\tilde{H}_2}^2 \simeq -0.03M_0^2 - 1.34M_{1/2}^2 + 1.5A_0M_{1/2} + 0.6A_0^2 \quad (13)$$

$$|\mu|^2 \simeq 0.03M_0^2 + 1.17M_{1/2}^2 - 2.0A_0M_{1/2} - 0.9A_0^2 \quad (14)$$

While the coefficients for the sleptons are of order unity, the coefficients c_j for the squarks grow very large, $c_j \simeq 5.0$, so that small errors in $M_{1/2}^2$ are magnified by nearly an order of magnitude in the solution for M_0 . By close inspection of Eqs.(8) for the Higgs mass parameter it turns out that the formally leading M_0^2 part is nearly cancelled by the M_0^2

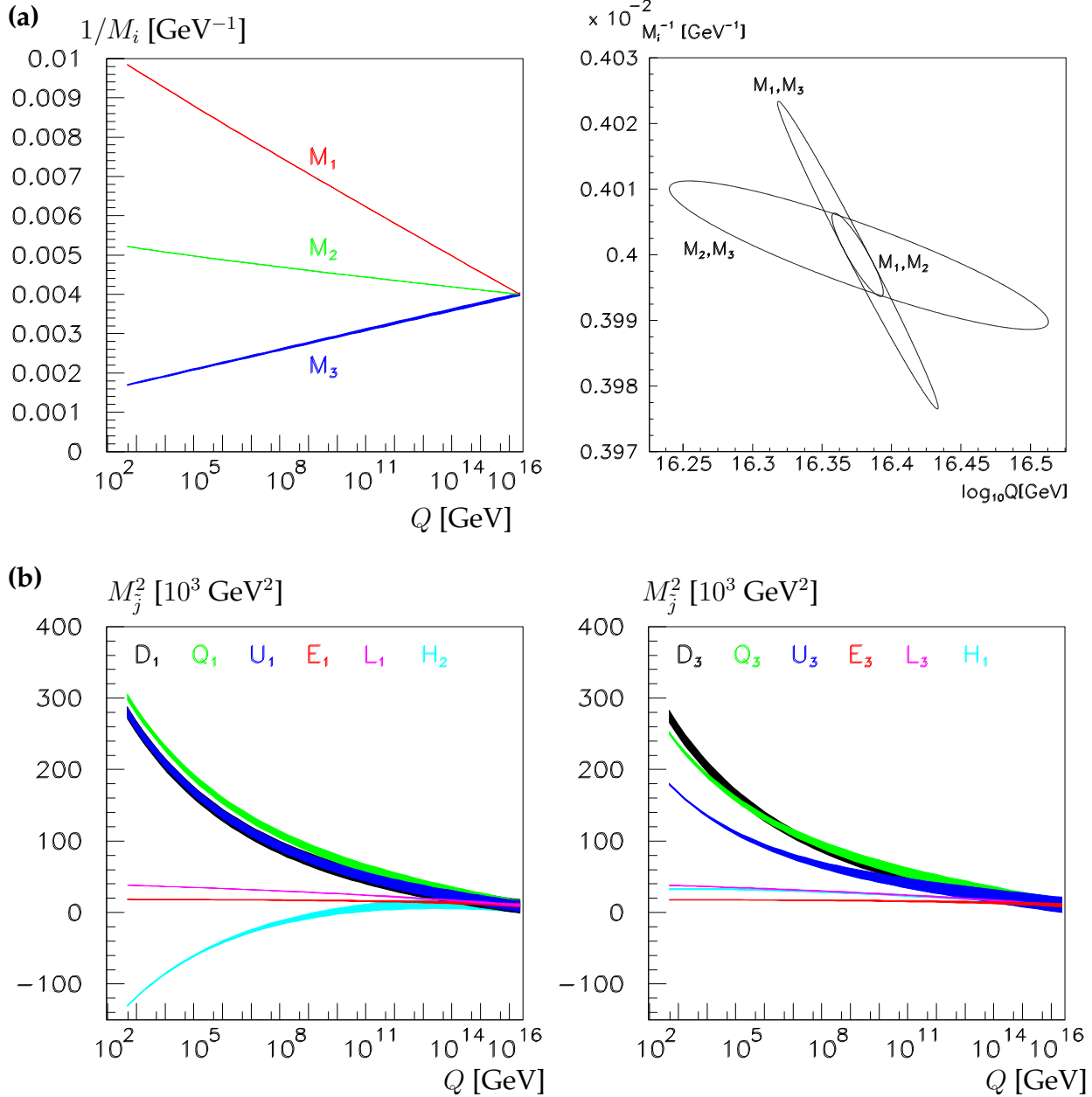


Figure 5: Evolution, from low to high scales, (a) of the gaugino mass parameters for “LHC+LC” analyses and the corresponding error ellipses of the universal GUT values; (b) left: of the first-generation sfermion mass parameters (second generation, dito) and the Higgs mass parameter $M_{H_2}^2$; right: of the third-generation sfermion mass parameters and the Higgs mass parameter $M_{H_2}^1$.

	Parameter, ideal	“LHC+LC” errors
M_1	250.	0.15
M_2	<i>ditto</i>	0.25
M_3		2.3
M_{L_1}	100.	6.
M_{E_1}	<i>ditto</i>	12.
M_{Q_1}		23.
M_{U_1}		48.
M_{L_3}		7.
M_{E_3}		14.
M_{Q_3}		37.
M_{U_3}		58.
M_{H_1}	<i>ditto</i>	8.
M_{H_2}		41.
A_t	-100.	40.

Table 7: Values of the SUSY Lagrange mass parameters after extrapolation to the unification scale where gaugino and scalar mass parameters are universal in mSUGRA [mass units in GeV].

part of $c'_{j,\beta} \Delta M_\beta^2$. Inverting Eqs.(8) for M_0^2 therefore gives rise to large errors in the Higgs case. Extracting the trilinear parameters A_k is difficult and more refined analyses based on sfermion cross sections and Higgs and/or sfermion decays are necessary to determine these parameters accurately.

A representative set of the final mass values and the associated errors, after evolution from the electroweak scale to M_U , are presented in Table 7. It appears that the joint “LHC+LC” analysis generates a comprehensive and detailed picture of the fundamental SUSY parameters at the GUT/PL scale. Significant improvements however would be welcome in the squark sector where reduced experimental errors would refine the picture greatly.

4 Summary

We have shown in this brief report that in supersymmetric theories stable extrapolations can be performed from the electroweak scale to the grand unification scale, close to the Planck scale. This feature has been demonstrated compellingly in the evolution of the three gauge couplings and of the soft supersymmetry breaking parameters, which approach universal values at the GUT scale in minimal supergravity. As a detailed scenario we have adopted the Snowmass reference point SPS1a. It turns out that the information on the mSUGRA parameters at the GUT scale from pure “LHC” analyses is too limited to allow for the reconstruction of the high-scale theory in a model-independent way. The coherent “LHC+LC” analyses however in which the measurements of SUSY particle properties at LHC and LC mutually improve each other, result in a comprehensive and detailed picture of the supersymmetric particle system. In particular, the gaugino sector

	Parameter, ideal	Experimental error
M_U	$2.36 \cdot 10^{16}$	$2.2 \cdot 10^{14}$
α_U^{-1}	24.19	0.05
$M_{\frac{1}{2}}$	250.	0.2
M_0	100.	0.2
A_0	-100.	14
μ	357.4	0.4
$\tan \beta$	10.	0.4

Table 8: Comparison of the ideal parameters with the experimental expectations in the combined “LHC+LC” analyses for the particular mSUGRA reference point adopted in this report [units in GeV].

and the non-colored scalar sector are under excellent control.

Though mSUGRA has been chosen as a specific example, the methodology can equally well be applied to left-right symmetric theories and to superstring theories. The analyses offer the exciting opportunity to determine intermediate scales in left-right symmetric theories and to measure effective string-theory parameters near the Planck scale.

Thus, a thorough analysis of the mechanism of supersymmetry breaking and the reconstruction of the fundamental supersymmetric theory at the grand unification scale has been shown possible in the high-precision high-energy experiments at LHC and LC. This point has been highlighted by performing a global mSUGRA fit of the universal parameters, c.f. Tab. 8. Accuracies at the level of per-cent to per-mille can be reached, allowing us to reconstruct the structure of nature at scales where gravity is linked with particle physics.

Acknowledgments

W.P. is supported by the ‘Erwin Schrödinger fellowship No. J2272’ of the ‘Fonds zur Förderung der wissenschaftlichen Forschung’ of Austria and partly by the Swiss ‘Nationalfonds’.

References

- [1] G. A. Blair, W. Porod and P. M. Zerwas, Phys. Rev. **D63** (2001) 017703 and Eur. Phys. J. **C27** (2003) 263; P. M. Zerwas *et al.*, Proceedings, Int. Conference on High Energy Physics ICHEP.2002, Amsterdam 2002.
- [2] I. Hinchliffe *et al.*, Phys. Rev. **D 55**, 5520 (1997); Atlas Collaboration, Technical Design Report 1999, Vol. II, CERN/LHC/99-15, ATLAS TDR 15.
- [3] TESLA Technical Design Report (Part 3), R. D. Heuer, D. J. Miller, F. Richard and P. M. Zerwas (*eds.*), DESY 010-11, hep-ph/0106315; American LC Working Group, T. Abe *et al.*, SLAC-R-570 (2001), hep-ex/0106055-58; ACFA LC Working Group, K. Abe *et al.*, KEK-REPORT-2001-11, hep-ex/0109166.

- [4] A. H. Chamseddine, R. Arnowitt and P. Nath, Phys. Rev. Lett. **49** (1982) 970; H. P. Nilles, Phys. Rept. **110** (1984) 1.
- [5] B. C. Allanach *et al.*, Eur. Phys. J. **C25** (2002) 113; N. Ghodbane and H.-U. Martyn, hep-ph/0201233.
- [6] D. N. Spergel *et al.* [WMAP Collaboration], Astrophys. J. Suppl. **148** (2003) 175.
- [7] H. Bachacou, I. Hinchliffe and F. E. Paige Phys.Rev. **D62** (2000) 015009.
- [8] B. C. Allanach, C. G. Lester, M. A. Parker and B. R. Webber, JHEP 0009 (2000) 004.
- [9] M. Chiorboli *et al.*, these proceedings.
- [10] F. Moortgat, these proceedings.
- [11] H.-U. Martyn and G. A. Blair, hep-ph/9910416.
- [12] A. Freitas, D. J. Miller and P. M. Zerwas, Eur. Phys. J. **C21** (2001) 361; A. Freitas, A. von Manteuffel and P. M. Zerwas, arXiv:hep-ph/0310182, Eur. Phys. J. in press.
- [13] A. Freitas *et al.*, Proceedings, Int. Conference on High Energy Physics ICHEP.2002, Amsterdam 2002.
- [14] S.Y. Choi, A. Djouadi, M. Guchait, J. Kalinowski, H.S. Song and P.M. Zerwas, Eur. Phys. J. **C14** (2000) 535.
- [15] S.Y. Choi, J. Kalinowski, G. Moortgat-Pick and P.M. Zerwas, Eur. Phys. J. **C22** (2001) 563 and Eur. Phys. J. **C23** (2002) 769.
- [16] H.-U. Martyn, Talk at the Prague Session of the ECFA/DESY Workshop, 2002 and Linear Collider Note LC-PHSM-2003-071.
- [17] H.-U. Martyn, these proceedings.
- [18] W. Porod, Comput. Phys. Commun. **153** (2003) 275.
- [19] F. James and M. Roos, Comput. Phys. Commun. **10** (1975) 343.
- [20] K. Inoue, A. Kakuto, H. Komatsu, and S. Takeshita, Prog. Theor. Phys. **68**, 927 (1982); Erratum, *ibid.* **70**, 330 (1983).
- [21] S. Martin and M. Vaughn, Phys. Rev. **D50**, 2282 (1994); Y. Yamada, Phys. Rev. **D50**, 3537 (1994); I. Jack, D.R.T. Jones, Phys. Lett. **B333** (1994) 372.
- [22] J. Bagger, K. Matchev, D. Pierce, and R. Zhang, Nucl. Phys. **B491** (1997) 3.
- [23] G. Degrassi, P. Slavich and F. Zwirner, Nucl. Phys. **B611** (2001) 403; A. Brignole, G. Degrassi, P. Slavich and F. Zwirner, Nucl. Phys. **B631** (2002) 195; Nucl. Phys. **B643** (2002) 79; A. Dedes and P. Slavich, Nucl. Phys. **B657** (2003) 333; A. Dedes, G. Degrassi and P. Slavich, hep-ph/0305127.

- [24] S. Dimopoulos, S. Raby and F. Wilczek, Phys. Rev. **D24** (1981) 1681; L. E. Ibanez, G. G. Ross, Phys. Lett. **B105** (1981) 439; U. Amaldi, W. de Boer and H. Fürstenau, Phys. Lett. **B260** (1991) 447; P. Langacker and M. Luo, Phys. Rev. **D44** (1991) 817; J. Ellis, S. Kelley, D. V. Nanopoulos, Phys. Lett. **B260** (1991) 161.
- [25] S. Weinberg, Phys. Lett. **B91** (1980) 51; L.J. Hall, Nucl. Phys. **B178** (1981) 75.
- [26] G.G. Ross and R.G. Roberts, Nucl. Phys. **B377** (1992) 571; H. Murayama and A. Pierce, Phys. Rev. **D65** (2002) 055009.
- [27] H. Hagiwara *et al.* [Particle Data Group Collaboration], Phys. Rev. **D66** (2002) 010001-1.
- [28] K. Mönig, in “Physics and Experiments with Future Linear e^+e^- Colliders”, eds. A. Para, H.E. Fisk, Melville 2001, hep-ex/0101005.
- [29] J. Erler, S. Heinemeyer, W. Hollik, G. Weiglein and P.M. Zerwas, Phys. Lett. **B486** (2000) 125.
- [30] B. C. Allanach, S. Kraml and W. Porod, JHEP **0303** (2003) 016; see also <http://cern.ch/kraml/comparison/>